Journal of Applied Polymer Science

Role of processing history on the mechanical and electrical behavior of melt-compounded polycarbonate-multiwalled carbon nanotube nanocomposites

Gabriel Yew Hong Choong,[1] Chun Yee Lew,[2] Davide Stefano Antonio De Focatiis[1]

[1]Division of Materials, Mechanics, and Structures, Faculty of Engineering, University Of Nottingham, Nottingham NG7 2RD, United Kingdom

[2]Nanocyl S.A., Sambreville B-5060, Belgium

Correspondence to: G.Y.H. Choong (E-mail: Gabriel.Choong@nottingham.ac.uk)

ABSTRACT: This work investigates the effects of primary compounding temperature and secondary melt processes on the mechanical response and electrical resistivity of polycarbonate filled with 3 wt % multiwalled carbon nanotubes (CNT). Nanocomposites were melt compounded in an industrial setting at a range of temperatures, and subsequently either injection molded or compression molded to produce specimens for the measurement of electrical resistivity, surface hardness, and uniaxial tensile properties. Secondary melt processing was found to be the dominant process in determining the final properties. The effects observed have been attributed to structural arrangements of the CNT network as suggested by morphological evidence of optical microscopy and resistivity measurements. Properties were found to be relatively insensitive to compounding temperature. The measured elastic moduli were consistent with existing micromechanical models. © 2015 Wiley Periodicals, Inc. J. Appl. Polym. Sci. **2015**, *132*, 42277.

KEYWORDS: extrusion; molding; polycarbonates; properties and characterization; structure-property relations

Received 1 September 2014; accepted 29 March 2015
DOI: 10.1002/app.42277

INTRODUCTION

The increasing miniaturization of electronic consumer products makes conductive polymers attractive for mass production. One important application area is packaging of sensitive electronics, where conductive containers are required to dissipate static charge. Carbon nanotubes (CNTs) are important candidate fillers, as they can both reinforce and add new functionalities to polymeric base matrices. The opportunity to exploit the high stiffness and strength of CNTs, in addition to their electrical conductivity, has been a subject of many industrial and academic studies. The solid-state properties of such filled thermoplastics are dependent on the processing history. The most widely used technique to disperse the filler industrially is melt processing, consisting of a primary process such as compounding/extrusion, and a secondary or forming process such as injection molding (IM) or compression molding (CM).

Prior to melt mixing with a polymer, initial "as-produced" CNT agglomerates are called primary agglomerates, and consist of linear dimensions ranging from 1 μm through to in excess of 675 μm, depending on the CNT manufacturer.[1] The shear stress generated during mixing is used to decrease the size of these agglomerates and to disperse them into the melt. The difficulty in turning these primary agglomerates into well dispersed nanotubes comes from the physical entanglements and van der Waals forces between the individual CNTs.[2] Reagglomeration can also take place during melt processes, when the nanotubes flocculate due to the same forces, and these are known as secondary agglomerates.

When the addition of filler to the matrix reaches a critical loading content, a continuous conductive path is formed, resulting in an abrupt change in the material behavior. This loading content is identified as the percolation threshold. Electrical resistivity has been typically used to identify this threshold in CNT-filled thermoplastics.[3,4] The dependence of electrical conductivity of thermoplastic-CNT nanocomposites during melt deformations was investigated by Alig *et al.* using simultaneous rheology and electrical resistivity measurements,[5] and they postulated that there is competition between the shear-induced destruction and formation of a CNT network. The same group also highlighted that secondary agglomeration of CNTs is a thermally activated process, also demonstrated by Jamali *et al.*[6] under quiescent conditions, which can be accelerated by shear flow. It is this same network that can provide the mechanical reinforcement of a CNT-thermoplastic system, as well as the necessary electrical conductivity. However, achieving uniform CNT

dispersion in the matrix through polymeric melt processes remains challenging. If specific electrical properties are required, then the filler concentration must be above the percolation threshold, but this in turn increases the likelihood of CNT agglomeration. Hence, there is a need to investigate how existing processing methods can be tailored to control the final properties of percolated CNT-thermoplastic systems for conductive packaging applications.

Several detailed studies on the influence of small batch mixing conditions on polycarbonate-multiwalled carbon nanotubes (PC-MWCNT) have been reported in the literature.[2,3,5,7,8] These provide insights into the complex mixing taking place during commercial processes, although batch mixers have different flow conditions (stresses and velocity fields) to extruders. In a percolated system, Kasaliwal *et al.* observed that an increase in mixing speed resulted in a significant increase in macrodispersion (i.e., dispersion of CNT agglomerates at a macroscopic scale), but in only minor changes to the levels of resistivity, regardless of the melt compounding temperature.[7] This suggests that (1) the formation of a conductive CNT network, and (2) the process of dispersing CNT primary agglomerates may occur via different mechanisms.[7]

Both Pegel *et al.* and Kasaliwal *et al.* reported that a lower melt temperature (and hence higher matrix viscosity) improves CNT dispersion.[2,7] This implies that rupture of agglomerates necessary to disperse the CNTs in the matrix is primarily controlled by matrix viscosity. However, CNT network formation is enhanced by a matrix of lower molar mass and by processing at higher temperature.[9] The generally agreed view is that a CNT network consists of weakly bonded clusters that break up and reagglomerate to form a conductive pathway during the application of shear, which suggests that the destruction of CNT-CNT bonds is reversible.

The evidence in the literature points to an increasing electrical conductivity in CNT–polymeric systems with increasing CNT agglomeration.[2,5,9] Kasaliwal *et al.* observed in PC-MWCNT (1 wt %) that low electrical resistivity is achieved when the mean diameter of undispersed agglomerates is less than 100 μm, with most agglomerates in the range of 1–10 μm.[10] In contrast to this, the enhancement of mechanical properties of the same systems arises from the presence of well dispersed individual CNTs, from their outstanding tensile properties, and from the large surface to volume ratio of individual tubes. Isolated nanotubes increase the CNT surface area available for wetting by the matrix, leading to an increase in CNT-matrix interaction, and facilitates efficient load transfer from the matrix to the CNTs. Therefore, while electrical properties of PC-MWCNTs stem from the formation of a CNT network structure, improvements in mechanical properties are achieved with good dispersion of individual CNTs in the matrix.

IM is a conventional process used to produce high volumes of complex parts, as required in the electronics packaging industry. Several studies have been performed to understand the complex effects of IM parameters on the final properties of percolated PC-CNT nanocomposites.[11–14] These all agree that melt temperature and injection velocity has a significant role in determining the electrical behaviour, and highlight the effect of a skin layer in which oriented CNTs were observed and a disrupted filler network could be inferred through an increase in electrical resistivity.[5,11,13–15] Compression moulding is generally a lower volume production method, but is preferred to enhance electrical properties because the timescales involved promote the build-up of an isotropic CNT network structure. This was observed by Kasaliwal *et al.* who studied and observed the effects of pressing speed, pressing time, and melt temperature on 1 wt % PC-MWCNT, but no significant influence on percolated 2 wt % PC-MWCNT.[7]

The effect of compounding parameters in an industrial setting on CNT thermoplastic systems have not been investigated in detail, perhaps understandably due to the significance of thermal and shear history of secondary process on final properties of a nanocomposite part. Commercially, nanocomposites are frequently delivered as compounded granulated feedstock to manufacturers, who re-melt the granules using standard polymer processes to form their products. Pegel *et al.* observed that formation of secondary agglomerates from initially dispersed MWNTs can decrease electrical resistivity.[2] However, in Jamali *et al.*'s study on a well dispersed MWCNT-filled polypropylene (PP) system that was subsequently heated and re-processed, extensive reagglomeration was observed with particle analysis, that eventually led to a rise in electrical resistivity.[6] Hence, feedstock compounders play a role in the dispersion of the primary agglomerates that may influence secondary agglomeration in the forming process. In 2010, Mack *et al.* varied extrusion screw speed, throughput and screw configuration during compounding of PC-MWCNT, and subsequently injection molded specimens to shape.[16] They found that the extrusion parameters did not significantly affect either the electrical resistivity of PC filled with >1 wt % CNT or the mechanical properties (tensile properties and impact strength) of PC filled with <5 wt % CNT.

Most of the research on PC-MWCNT to date has been focused primarily on materials produced in laboratory environments using small scale laboratory extruders. This work is instead focused on materials produced using industrial scale equipment, and separately explores the roles of compounding temperature, T_c (used to produce feedstock), and of the type of the secondary molding process (that dictates the final bulk properties) on a typical percolated PC-CNT system. As will be shown, it is the type of secondary melt process that dominates the final electrical and mechanical properties. The same properties are somewhat insensitive to variations of temperature in the primary compounding process. This suggests that there is flexibility in industrial process parameters for compounding the feedstock to cater for the demands of products produced by different secondary melt processes.

EXPERIMENTAL

Materials

The matrix polymer used was Makrolon 2205 (Bayer Material Science AG, Germany), a low viscosity grade PC with a melt mass-flow rate of 37 g 10 min^{-1} according to the manufacturer's data sheet,[17] and glass transition temperature (T_g) of ~146°C.[18] The nanotubes used were Nanocyl NC7000

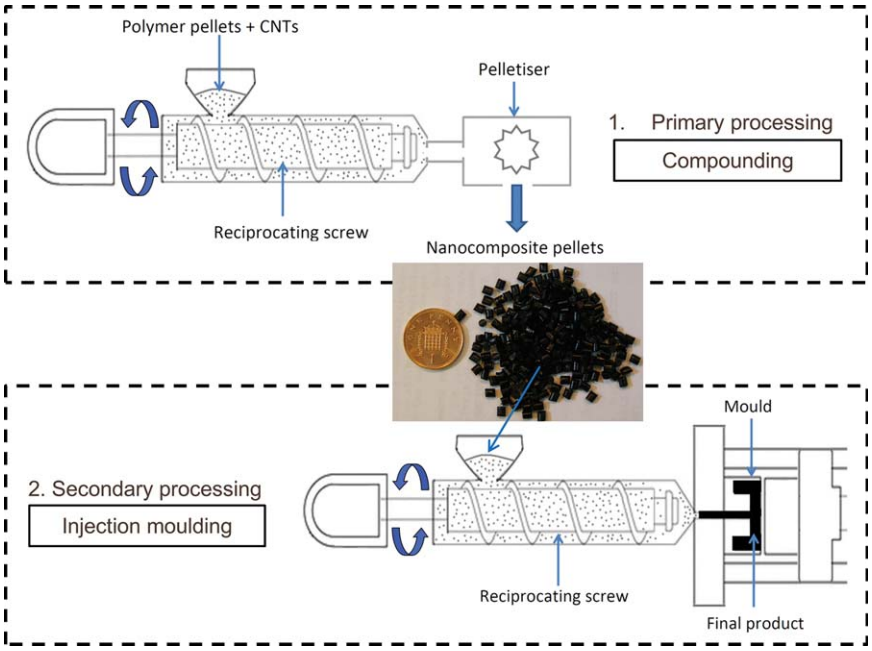

Figure 1. Schematic diagram of the primary (compounding) and the secondary process (IM shown) applied to the PC filled with 3 wt % multiwalled carbon nanotubes used in this study. The other secondary process used was CM (not shown). [Color figure can be viewed in the online issue, which is available at wileyonlinelibrary.com.]

multiwalled CNTs, manufactured by Nanocyl S.A., via a catalytic chemical vapor deposition process. Nanotubes have a mean outer diameter of 10 ± 3 nm, a median length of 1300 nm and primary agglomerate sizes of 675 μm and above.[1,19]

Specimen Preparation

Nanocomposite Compounding. A range of PC-MWCNTs were melt compounded by Nanocyl S.A. using an Industrial Leistritz ZSK-27 MAXX corotating twin-screw extruder with a proprietary screw profile with a length to diameter ratio of 48 : 1. The heated barrel was divided into 11 temperature zones. Seven different masterbatches were produced with variations in the barrel temperature profile. For all extrusions, the temperatures at zones 1, 2, 11 and at the die were fixed at 250, 270, 290, and 300°C, respectively, and a single temperature was specified for zones 3–10, and varied between 230 and 290°C in 10°C increments. MWCNTs were gravimetrically fed into the PC melt through a twin–screw side feeder at zone 4, at a nominal mass fraction of 3 wt % for all PC resins. The extrusion screw speed was fixed at 300 rpm. The extrudate was pelletized using a standard industrial rotary gear cutter adjusted to run at speed of 30 rpm to cut the extrudate into approximately cylindrical granules (Ø =2.5 × 3 mm) for subsequent secondary forming processes. Figure 1 illustrates the two stage process of compounding (primary process) and of forming (secondary process) employed for the materials in this study.

Compression Molding. Part of the compounded nanocomposite granules were dried in an air-circulating oven at 80°C for a minimum of 8 h prior to CM. Dumb-bell shaped specimens of dimensions 75 × 5 × 2 mm^3, corresponding to type 1BA of the British Standard BS EN ISO 527-2:2012,[20] were compression molded using a Daniels heated press and a custom flash mold[21] consisting of interlocking parts to produce the cavity shape. This design of mould eliminates postmolding specimen preparation. Moulding was performed at 250°C. The procedure consisted of a warm up period, a 5 min stage where pressure was applied and released repeatedly to dislodge any trapped air, holding for a further 5 min at the molding temperature to allow relaxation of the polymer, and a cooling stage where cold water is flushed through channels in the heated platens, producing a repeatable cooling rate of ~20°C min^{-1} through to a temperature sufficiently below T_g.

Injection Molding. Another part of the compounded granules was used in IM, using an Engel Victory 80 (after drying) with the parameters given in Table I. Dumb-bell shaped specimen moulds were employed in accordance with ASTM D638 (approximate dimensions 150 × 10 × 4 mm^3). The linear dimensions of the IM specimens are twice those of the CM specimens.

Optical Microscopy

Macrodispersion of CNT agglomerates formed after primary and secondary processing was explored using thin 2 μm sections

Table I. IM Conditions for PC-MWCNT (3 wt %)

Parameter	Values
Injection temperature (nozzle)	300°C
Plasticizing speed	0.4 m s^{-1}
Mold temperature	120°C
Back pressure	40 bar
Hold pressure	450 bar
Hold cycle time	8 s

prepared from PC-MWCNT (3 wt %) IM and CM bars using a RMC PT-PC Power Tomes ultramicrotome with a glass knife. Representative sections from both secondary processes were obtained from the cross-sections of the gauge lengths of the tensile bars to study the core region morphology. Optical microscopy investigations were conducted using an Olympus BX 51 transmission microscope fitted with a 10× objective and a Q-imaging camera was used to record the images.

To quantify the morphology of the specimens, digital image processing was used to apply background corrections and to decrease the influence of defects (e.g., scratches) from sectioning. Image processing was performed with ImageJ software following the procedure proposed by Pegel *et al.*[22] In addition, sections of the images that included obvious artefacts persisting after the binarisation and the application of a morphological filter were removed manually. This process therefore allows particle identification of all agglomerates with areas of 7.9 μm^2 and above, equivalent to perfectly circular particles with a diameter $>\sim 3$ μm. ImageJ was also used to perform particle analysis. The cumulative area of images evaluated for each secondary process was above 3 mm^2, and a minimum of 5 sections were taken along the length of each tensile bar.

Macrodispersion of the CNT agglomerates was calculated as an index based on a method developed for the rubber industry, and previously employed for several MWCNT–filled thermoplastic systems.[7,23,24] The macrodispersion index D is expressed as

$$D = \left(1 - f\frac{(A/A_0)}{v}\right) \times 100\% \quad (1)$$

where A/A_0 is the ratio of the accumulated area of agglomerates to the total micrograph area, known as the agglomerate area fraction; f is the packing density of CNTs (a value of 0.25 is employed following literature for CNTs[7,23,24]), and v is the volume fraction of the filler (assuming a CNT density of 1.75 g cm^{-3}). When A/A_0surpasses 8.4% for a CNT loading content of 3 wt % (2.1 vol %), then D becomes zero, implying the worst possible state of dispersion. D = 100% implies that no agglomerates $\geq$7.9 μm^2 are visible, and hence represents a state of well dispersed CNTs.

Electrical Resistivity Measurements

Volume resistivity of PC-MWCNT specimens were measured using an in-house two–terminal fixture with spring-loaded terminal contacts.[25] Contacts are made of conductive carbon–filled silicone (Laird Technologies C5–9134) to promote intimate contact with the rigid surfaces of the specimens. The spring-loaded contacts applied a constant pressure of 70 kPa at each end of the specimen.

Contact resistivity, ρ_c, was determined by means of the extrapolation method using surface terminal contacts.[26] The method involves measuring the voltage distribution along a constant cross section of a rectangular bar (100 × 6 × 1 mm^3) and determination of the contact resistance by extrapolation of the voltage to zero contact spacing, thus eliminating the effect of contact resistance.

To perform a comparative study between CM and IM specimens, the voltage per unit length was fixed at 143 V m^{-1}. A constant voltage was applied for 20 s using the built-in voltage source of a Keithley 6517B electrometer, during which time the current was logged using the same instrument. The volume resistivity, ρ, is obtained from the time-averaged volume resistance, R_v, as $\rho = R_v A/d$, where A is the specimen cross sectional area and d is the distance between the terminals. Five specimens were measured for each forming method and each T_c. All measurements were performed at ambient temperature and corrected for contact resistance.

The Tietjen-Moore's outlier test[27] was used to detect and remove small numbers of outliers in the experimental data at a 5% significance level. Error bars shown in the results represent two standard errors. The same specimens were employed for electrical resistivity followed by indentation and tensile testing.

Mechanical Measurements

The Vickers hardness method (HV) was employed to determine the surface hardness of the specimens. The procedure employs a diamond pyramidal indenter with a square base. A minimum of four indentations were performed on the grip area of each dumb-bell shaped specimen, giving a total of 20 measurements for each forming method and T_c. A load of 5 kgf was applied for 15 s, typically yielding a penetration of ~0.16 mm. The hardness was calculated as the arithmetic mean of the diagonal lengths of the indentations measured using an ocular device. The position of the indentations was ensured to be at least 2.5 indentation diagonal lengths l_d from the edge of each specimen, and the distance between repeated indentations was at least $3l_d$.

Tensile testing was performed at room temperature using an Instron 5968 equipped with 5 kN load cell. Tests were performed to failure at a fixed strain rate of 5.56 × 10^{-4} s^{-1}, corresponding to cross head speeds of 1 and 2 mm min^{-1} for CM and IM specimens, respectively. Due to the difference in gauge lengths between CM and IM specimens, strain was measured using either a 25 or a 50 mm gauge length clip-on extensometer accordingly. Five specimens were tested for each forming method and T_c. Young's modulus, E, was determined by linear regression between 0.1 and 0.45% strain for nanocomposites, and between 0.1 and 1.0% for CM unfilled PC. Unfilled IM PC bars were not available for analysis.

RESULTS AND DISCUSSION

Morphology of Specimen Core Region after Secondary Melt Processing

Figure 2(a,b) show representative optical micrographs of the cross-section of PC-MWCNT (3 wt %) CM and IM tensile bars, respectively. An example of the binary image used for particle identification is shown in Figure 2(c), corresponding to the micrograph from Figure 2(a). Agglomerates of various sizes can be seen in both micrographs. Figure 2(d) shows a normalized frequency histogram of particle area. IM sections have generally a higher number of particles with areas of more than 120 μm^2 compared with CM sections. The mean particle areas are 130.3 ± 18.7 μm^2 and 150.8 ± 21.2 μm^2 for CM and IM sections, respectively.

The average macrodispersion index D calculated using eq. (1) is 33% for CM sections, whereas for IM sections it is 70%. This

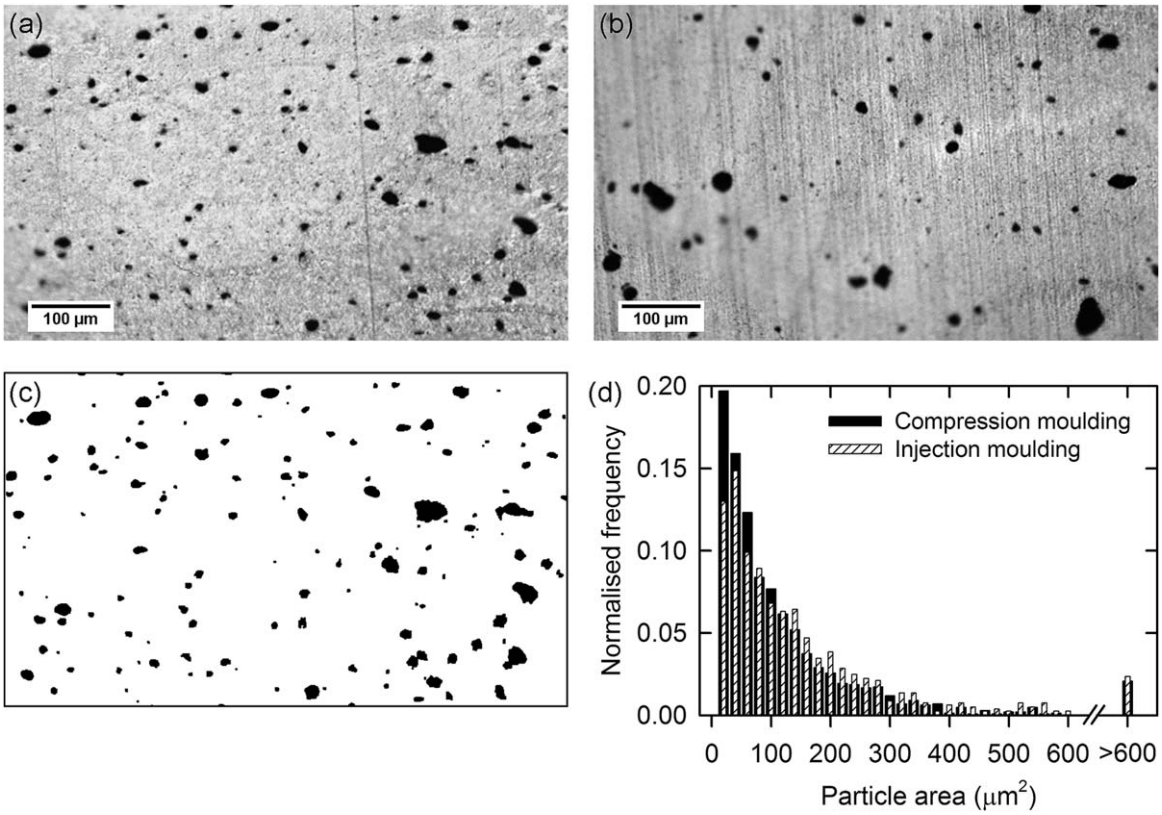

Figure 2. Optical micrographs of PC-MWCNT (3 wt %) sections ($t = 2$ μm) obtained from the gauge length of (a) CM and (b) IM tensile bars. Background correction and binarisation of (a) produces image (c). Normalized frequency histogram of particle area for all micrographs of CM and IM samples (d).

indicates that IM bars have a better state of CNT agglomerate dispersion at a scale of <7.9 μm^2 when compared with CM specimens.

Electrical Resistivity

Figure 3 presents the volume resistivities of CM and IM bars as a function T_c. Two CM specimen measurement outliers and three IM specimen outliers were rejected from the data set. The most striking difference in resistivity is between secondary processes: ρ of CM bars is consistently lower than that of IM bars by one order of magnitude. The overall average ρ of CM and IM PC-MWCNT 2205 across T_c are 1.26 ± 0.28 and 12.20 ± 1.62 Ω m, respectively.

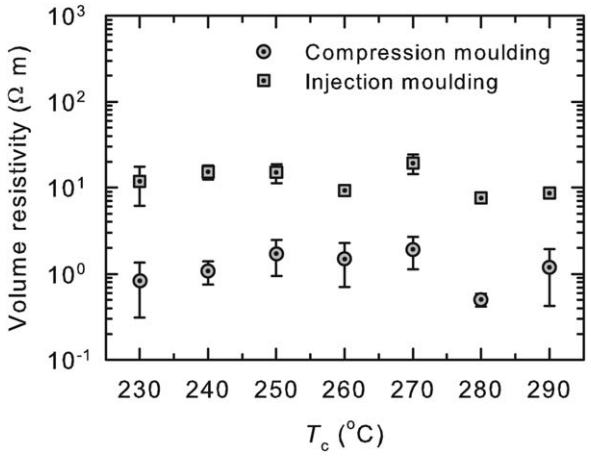

Figure 3. Electrical volume resistivity of PC-MWCNT 2205 (3 wt %) compounded at temperatures between 230 and 290°C, and subsequently formed to shape by CM and IM.

The order of magnitude difference in resistivity between IM and CM specimens can be explained by considering the timescales available for CNT reagglomeration.[7] Flocculation experiments (oscillatory shear at fixed frequency under isothermal conditions) have shown that the formation of the CNT network in PC melts evolves with time.[28] The increased time for relaxation in the flash mould at relatively high temperature allows the formation of a more percolated network in the CM bars, resulting in lower resistivity levels relative to IM bars. Polymer mobility was shown by these authors to be the dominant relaxation mechanism in these nanocomposites, and therefore can be associated with the greater degree of CNT reagglomeration.[18]

Kasaliwal *et al.* hypothesized three different percolated structure arrangements for low electrical resistivity: (1) cluster–cluster percolation, (2) combination of small agglomerates and dispersed CNTs, and (3) a network of well-dispersed CNTs.[8] The systems in this work exhibit morphology and properties indicative primarily of arrangement (2), but with different degrees of agglomeration and dispersion. Figure 4 shows two such plausible morphologies based on evidence from both the micrographs in Figure 2 and the electrical measurements, with Figure 4(a)

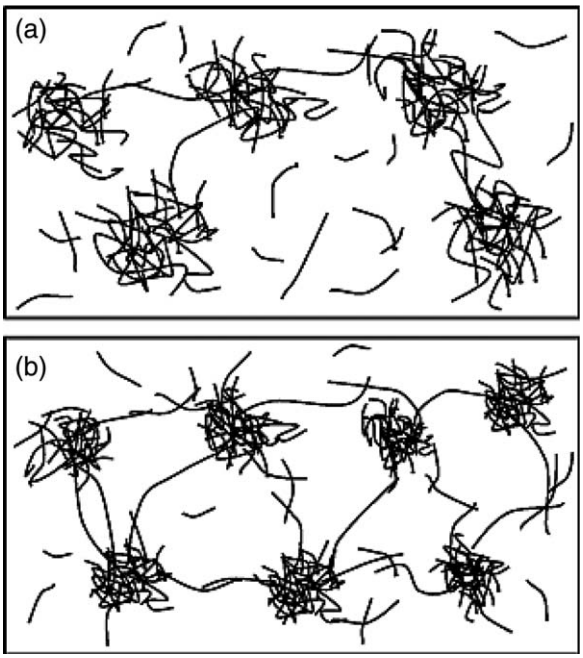

Figure 4. An illustration of structural arrangements of CNT agglomerates with different levels of dispersion and percolation: (a) larger agglomerates with fewer intercluster connections (and hence a less conductive network); and (b) smaller agglomerates with more intercluster connections (and hence a more conductive network).

representing the IM morphology ($D = 70\%$) and Figure 4(b) the CM morphology ($D = 33\%$). Although the IM morphology displays a better dispersion index, its larger agglomerates are less well connected and give rise to a higher electrical resistivity when compared to the CM morphology. To a lesser degree, within an IM process, CNT orientation has been observed in transmission electron micrographs[13,15] and the conductive network was reported as disrupted.[11,13,14] These effects lead the formation of a skin layer with increased resistivity relative to the bulk.

The resistivity values obtained in this work are consistent with those measured by Spikowski and Kunzelman[29] on CM specimens of a comparable nanocomposite system using a similar surface contact two-terminal measurement method, and also with resistivity values reported by Mack *et al.* on similar IM specimens,[16] as shown in Table II. It is worth noting, however, that in IM specimens differences of up to 10 orders of magnitude in resistivities have also been reported in the literature on comparable PC-MWCNT (3 wt %) systems.

The same trend of an increase in resistivity with T_c followed by a decrease at 280°C and an increase at 290°C was observed by Lew *et al.*[30] on nanocomposite extrudate compounded at identical temperatures as investigated here. The magnitudes of the resistivity values measured by Lew *et al.* differ to those measured here, which could be due to differences in the resistivity measurement techniques, and in the secondary processing. The same group found that compounding at 280 and 290°C yielded the highest and lowest shear viscosities, respectively, for the range of shear rates between 100 and 5000 s^{-1} (and hence relevant to primary and secondary processing), although the variation was not very significant.[30] They reported that the lowest electrical resistivity occurs with the highest shear viscosity, suggesting that at high shear viscosity the stress breaks-up the initial primary MWCNT agglomerates into smaller agglomerates, most likely via a rupturing mechanism.[7]

Other studies have also found electrical resistivity to be relatively insensitive to macrodispersion. Jamali *et al.* found that re-processing a PP–MWCNT (4 wt %) at a high shear rate (3000 s^{-1}) after a quiescent hold increased both CNT macrodispersion and electrical conductivity independently of the initial compounding shear rate (100 and 3000 s^{-1}).[6] Here, resistivity decreased to a plateau even when increasing re-processing residence time that produced a higher macrodispersion. Similarly, Kasaliwal *et al.* observed only small changes (one order of magnitude) in the volume resistivity with macrodispersion indices D of ~30 and ~70% (for a percolated PC-MWCNT 1 wt % system).[7] These macrodispersion indices and changes in resistivity are consistent with those reported in this work.

Overall, resistivity was not significantly affected by variation in the T_c, in both secondary processes. This is in contrast with the work of Kasaliwal *et al.* who reported that high temperatures are favorable for obtaining lower resistivity, when mixing in a laboratory extruder.[7] They observed a reduction of 10 orders of magnitude in ρ as T_c increased from 240 to 260°C in CM PC-MWCNT (1 wt %). This suggests that their systems changed from unpercolated to percolated as a consequence of the effect of T_c on the reduced CNT loading. In our study, all systems are percolated independently of variations in T_c and in secondary process, consistent with the reported percolation threshold of 0.5–2.0 wt %.[3,4]

Surface Hardness

Figure 5 reports measurements of Vickers hardness as a function of T_c for both IM and CM specimens. Hardness of CM specimens is systematically higher than that of IM specimens, by 1–3%.

The overall average of HV for CM specimens is 15.4 ± 0.1 kgf mm^{-2}, and for IM specimens is 15.0 ± 0.2 kgf mm^{-2}. All IM bars recorded a lower hardness than the equivalent CM nanocomposites. Although these differences are not highly significant, they are likely due to the less well-established nanotube

Table II. Literature Values of Electrical Resistivity of PC-MWCNT (3 wt %) Determined with the Two-Terminal Method and Comparison with This Work

Secondary process	Volume resistivity (Ω m)	References
CM	~0.4 - 1.6	29
	~0.5 - 1.9	This work
IM	10^8 - 10^{10}	12
	10^3 - 10^7	29
	~0.7 - 20	16
	~0.9 - 12	11
	~8 - 19	This work

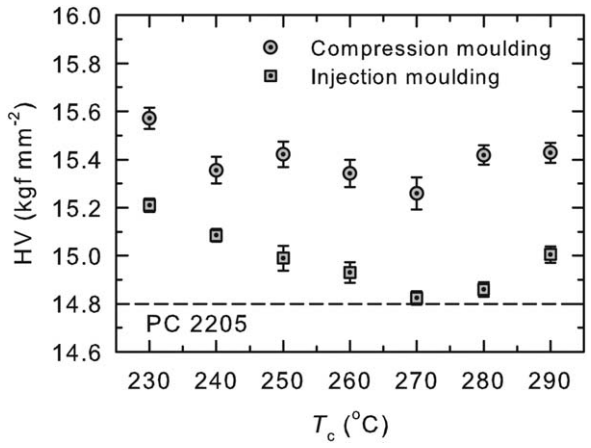

Figure 5. Vickers hardness of CM and IM PC-MWCNT 2205 compounded at temperatures between 230 and 290°C. The dashed line represents the Vickers hardness of unfilled CM PC 2205.

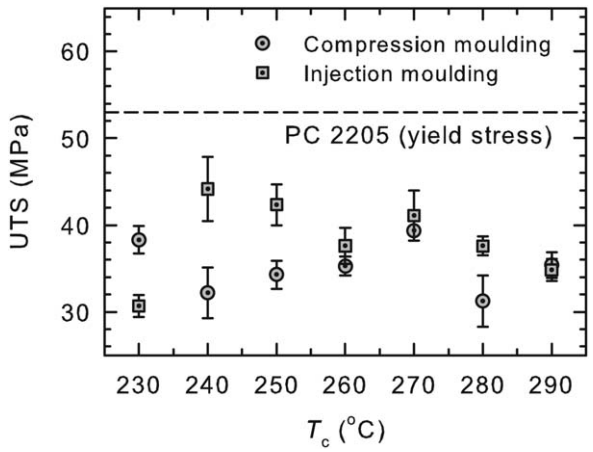

Figure 7. UTS of CM and IM PC-MWCNT 2205 compounded between 230 and 290°C. The dashed line represents the yield stress of unfilled CM PC 2205.

network in IM specimens near the surface (i.e., skin layer), where other studies have observed oriented individual CNTs.[13,15]

All the nanocomposite bars, regardless of the type of secondary process, produced higher HV than the unfilled CM PC 2205, measured as 14.8 ± 0.1 kgf mm^{-2}; but this difference is again minor (1–4%). This increase in HV is attributed to the presence of CNTs that stiffen the surrounding matrix. Liu *et al.* reported an 11% increase in Shore hardness for CM PC-MWCNT (3 wt %) relative to the unfilled material, in a similar but not identical material and process.[31] The smaller hardness difference in this study could be attributed to (1) poor interfacial bonding between the CNTs and the polymer chains resulting in ineffective stress transfer and (2) agglomeration of the CNTs leading to soft matrix–rich regions. Such CNT agglomerates are clearly visible in Figure 2(a,b).

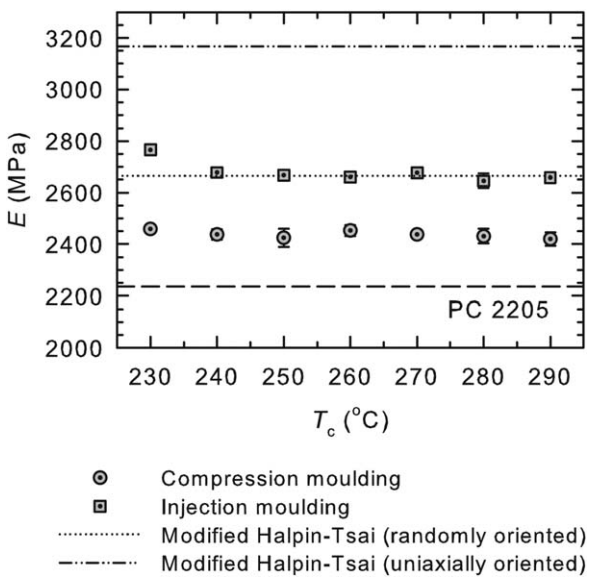

Figure 6. Young's moduli of CM and IM PC-MWCNTs 2205 compounded between 230 and 290°C. The dashed line represents the unfilled CM PC 2205. The dotted line represents Thostenson and Chou's[32] modified Halpin-Tsai equation for randomly oriented CNTs whereas the dot-dot-dash line represents Gojny *et al.*[33] modified Halpin-Tsai equation for perfectly oriented CNTs.

Tensile Properties

The effect of T_c on elastic modulus is presented in Figure 6 for both IM and CM specimens. The moduli of IM specimens are consistently higher than those of CM specimens for the range of T_c investigated. The moduli of CM specimens range between 2420 and 2459 MPa, and those of IM specimens between 2645 and 2765 MPa, corresponding to a difference of 5% between minimum and maximum measured values within each set. The modulus of unfilled CM PC was measured as 2236 ± 2 MPa. The addition of CNTs increased the modulus by up to ~10%.

The presence of stiff nanotubes within the nanocomposite contributes to the observed increase in modulus. In IM specimens, the additional increase relative to CM specimens could be attributed to (1) the frozen-in orientation of the polymer chains, (2) the orientation of the CNTs, and (3) a different macrodispersion index *D*. We rule out polymer chain orientation, as its effects on IM PC are small.[34]

The effects of T_c on the ultimate tensile strength (UTS) are presented in Figure 7 for both IM and CM specimens. All nanocomposite specimens failed by brittle fracture while the stress was still rising, regardless of T_c or forming method, as shown in the representative stress–strain curves in Figure 8. This is in sharp contrast to the unfilled PC, which deforms in a ductile fashion with a yield followed by strain softening and subsequent hardening and failure at large strains.[34] The micrographs in Figure 2 and those published by one of the authors on identical PC-MWCNT (3 wt %)[11] suggest that significant agglomeration is present in these materials. The CNT agglomerates reduce the surface area of CNTs in contact with the polymer matrix, thus decreasing stress transfer efficiency, and may act as stress concentrators initiating fracture.

With the exception of the lowest and highest T_c, IM specimens failed at higher stresses than CM specimens, although differences are not large. Average UTS of CM and IM samples are

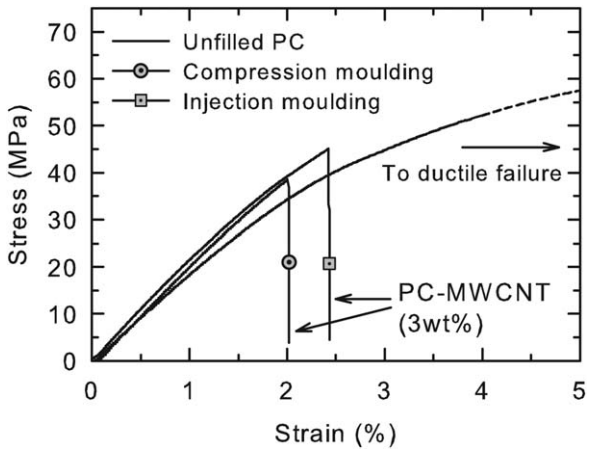

Figure 8. Representative stress-strain curves of CM and IM PC–MWCNT 2205 and unfilled CM PC 2205.

35.2 ± 1.7 and 38.3 ± 2.2 MPa respectively, whereas the average yield stress of unfilled CM PC is 53.0 ± 5.8 MPa.

Correlation Between Mechanical Response and Electrical Resistivity. To different degrees, solid-state properties of the nanocomposites were affected by both the primary process (through T_c) and by the type of secondary process (IM or CM). The effect of the secondary process is more apparent, and primarily due to the different timescales involved for the formation of the nanotube network. The effect of the primary process can appear to be overshadowed by the secondary process. For this reason, linear correlations between pairs of solid-state properties were investigated separately for IM and CM specimens.

The correlation coefficient, R, was determined between sets of pairs of measurements of resistivity, hardness, modulus, and UTS carried out on the same test specimens. Although none of the correlations are particularly strong, the most significant are between resistivity (considered on a logarithmic scale) and hardness for CM specimens and between elastic modulus and hardness for IM specimens. These correlation plots and correlation regression lines are shown in Figures 9 and 10 respectively. All other variables yielded weaker correlations ($|R| \leq 0.3$).

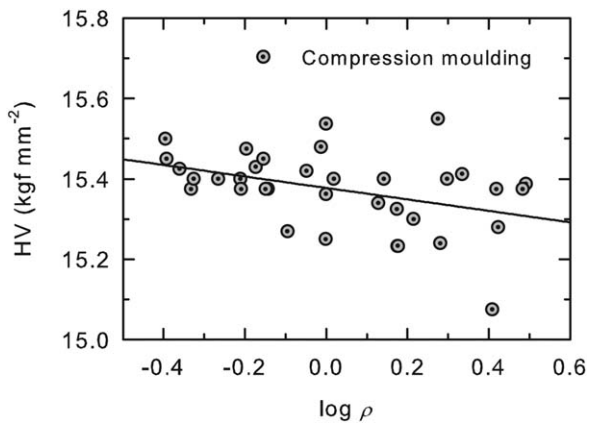

Figure 9. Relationship between surface hardness and log electrical resistivity for CM specimens, with linear regression, giving a correlation coefficient $R = -0.40$.

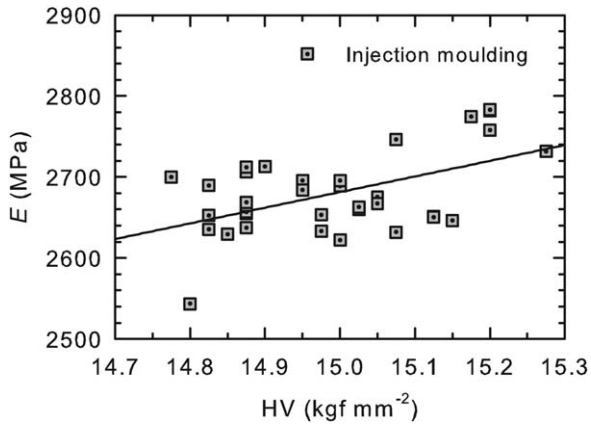

Figure 10. Relationship between Young's modulus and surface hardness for IM specimens, with linear regression, giving a correlation coefficient $R = 0.52$.

Figure 9 shows a slightly negative correlation between hardness and log resistivity in CM specimens, with $R = -0.40$. During CM, the extended relaxation times promote not only the formation of CNT agglomerates, but also a wider distribution of agglomerate size. The nature of this distribution will depend somewhat on the initial state of dispersion; since our PC-MWCNT systems are percolated, it is more favorable for the agglomerate size to increase, leading to a decrease in CNT agglomerate distribution that gives rise to both more matrix rich regions (i.e., lower hardness) and less conductive pathways (i.e., greater resistivity).

There is a small positive correlation between elastic modulus and surface hardness in IM specimens ($R = 0.52$), as shown in Figure 10. As observed in the literature for similar nanocomposites, the highest degree of CNT orientation during IM occurs on the surfaces of the moulded part.[13,15] Hardness can be interpreted as a measure of the residual plastic deformation after indentation, whereas modulus refers to the recoverable elastic stiffness. A nanocomposite system with a greater degree of CNT alignment near the surface contributes to a higher stiffness in the flow direction. Consider an indentation perpendicular to an individual CNT aligned along the flow direction: the CNT will appear more compliant since it is subjected to bending perpendicular to its axis. Surprisingly, Figure 9 shows the opposite effect: a positive correlation between E and HV. This could be explained since hardness is a record of only the plastic deformation: a greater hardness may be a sign of a greater elastic recovery for a given maximum indenter position. It is plausible to assume that bending CNTs will produce lower stress concentrations in the matrix than axially loading CNTs, and thus lead to a more elastic indentation that produces a smaller indent (i.e. greater hardness). Therefore increasing orientation in the flow direction could produce a material with both a stiffer axial modulus and a greater hardness in the perpendicular direction. Separate analysis of the indent diagonals in perpendicular directions was not able to resolve anisotropy of hardness, as might have been produced from flow-induced orientation of the nanofiller. At present, no other explanation is offered for this weak correlation.

Application of Models for the Prediction of Elastic Modulus

Micromechanical modeling is a commonly used technique to predict the modulus of traditional fiber reinforced composite systems. Several studies have approached nanocomposites in a similar manner, considering both randomly oriented and perfectly oriented nanotubes.[32,33,35] Typically, the filler particles are treated as solid cylinders or rods in macrofiber models. Since MWCNTs are hollow structures consisting of concentric cylinders of graphene, Thostenson and Chou modified the classical Halpin–Tsai equation for unidirectional fiber–reinforced composites to account for this by assuming that the outer CNT wall alone supports stress.[32] They expressed the modulus of a nanocomposite with perfectly aligned CNTs as

$$E = E_{\text{matrix}}\left(\frac{1+\frac{2l_{\text{CNT}}}{d_{\text{CNT}}}(\eta_{\text{L}}V_{\text{CNT}})}{1-(\eta_{\text{L}}V_{\text{CNT}})}\right)$$
$$\eta_{\text{L}} = \left(\frac{\frac{E_{\text{CNT}}}{E_{\text{matrix}}}-\frac{d_{\text{CNT}}}{4t}}{\frac{E_{\text{CNT}}}{E_{\text{matrix}}}+\frac{l_{\text{CNT}}}{2t}}\right) \quad (2)$$

where the CNT outer diameter is d_{CNT}, the length is l_{CNT}, the thickness of the outer wall is t, the volume fraction of CNTs is V_{CNT}, and E_{CNT} and E_{matrix} are the moduli of the nanotube and matrix respectively. Thostenson and Chou showed that this equation was in agreement with experimental measurements of modulus in stretched polystyrene-MWCNT films at both 5 and 10 wt % loading, and that the elastic modulus was particularly sensitive to CNT diameter.

The modified Halpin-Tsai equation was applied to obtain an estimate of modulus for the nanocomposites studied in this work. The constants used are $E_{\text{matrix}} = 2236$ MPa (measured from CM PC 2205), $E_{\text{CNT}} = 450$ GPa,[36] $l_{\text{CNT}} = 418$ nm, and $d_{\text{CNT}} = 10$ nm[19]; and $V_{\text{CNT}} = 0.021$ (determined using $\rho_{\text{CNT}} = 1.75$ g cm^{-3}). Using these values in eq. (2) produces a modulus of 3166 MPa. This is indicated by a dot-dot-dash in Figure 6 for comparison with IM materials. The average modulus for IM specimens was 2679 ± 17 MPa. The model overestimates the modulus by ~18%. Other systems have been compared to the modified Halpin–Tsai, which was found to either agree with or to overestimate the experimentally measured modulus.[35] An overestimation is to be expected since it is nearly impossible to obtain an IM specimen with perfectly aligned nanotubes.

Another possible explanation for the discrepancy is an overestimate of nanotube length, it is well known that a reduction in length (i.e., damage) occurs during melt compounding. Keeping other parameters constant, a length of 94.4 nm would produce the experimentally measured modulus, this would represent a decrease of ~77% relative to the original length value reported by Krause *et al.*[19] after extrusion. This is plausible considering different extruders and extrusion parameters were employed in the two studies. An alternative explanation is that the worm-like nature of CNTs results in shorter effective lengths when applied to a model that accounts for straight rod-like reinforcement. Finally, the model assumes perfect adhesion between polymer and filler. This is also unlikely since no CNT surface modification was employed in this work.

Gojny *et al.*[33] adapted Thostenson and Chou's approach to predict the modulus of a material filled with randomly oriented rod fillers as

$$E = E_{\text{matrix}}\left(\frac{3}{8}\left(\frac{1+\frac{2l_{\text{CNT}}}{d_{\text{CNT}}}(\eta_{\text{L}}V_{\text{CNT}})}{1-(\eta_{\text{L}}V_{\text{CNT}})}\right)+\frac{5}{8}\left(\frac{1+2(\eta_{\text{T}}V_{\text{CNT}})}{1-(\eta_{\text{T}}V_{\text{CNT}})}\right)\right)$$
$$\eta_{\text{T}} = \left(\frac{\frac{E_{\text{CNT}}}{E_{\text{matrix}}}-\frac{d_{\text{CNT}}}{4t}}{\frac{E_{\text{CNT}}}{E_{\text{matrix}}}+\frac{d_{\text{CNT}}}{2t}}\right) \quad (3)$$

where $\eta_{\text{L}}$is as in eq. (2). They reported good agreement between predicted and experimentally measured modulus for epoxy–CNT nanocomposites 0.1 wt %, but an overestimation with 1.0 wt %.

Equation (3) is employed on the materials used in this study, producing a modulus of 2664 MPa. This is shown as a dotted line in Figure 6. The value is ~10% higher than the average experimentally measured modulus of CM specimens, of 2412 ± 24 MPa. The discrepancy is likely due to invalid assumptions of uniformly dispersed fillers and perfect filler-matrix interface. In addition, the presence of small voids was identified in polished surface micrographs of both IM and CM specimens (not shown here).

Since IM specimens have a combination of aligned CNTs near the surface and more randomly oriented CNTs in the core, one may consider Thostenson and Chou's equation as an upper bound and Gojny's equation as a lower bound for the prediction of elastic modulus in IM specimens. The measured modulus of IM specimens is within this range, although the close proximity of the measured modulus to the lower bound suggests that, in the absence of other considerations, the orientation of the nanotubes may not be very significant.

CONCLUSIONS

This work has investigated the effect of primary compounding temperature, T_c, and of secondary process type (compression molding, CM, and injection molding, IM) on solid-state properties of percolated PC-multiwalled carbon nanotube, PC-MWCNT (3 wt %), nanocomposite systems, compounded in a commercial setting.

Resistivity of CM specimens was found to be an order of magnitude lower than that of IM specimens. This is consistent with a time-dependent build-up of a CNT network, most likely driven by polymer mobility that forms structural arrangements of connected CNT agglomerates with varying degrees of conductive pathways. The influence of the secondary process on the morphology of PC-MWCNT was evidenced by the quantification the state of CNT dispersion from optical micrographs, using particle size analysis leading to a macrodispersion index *D*. From this, it was determined that CM produced smaller agglomerates with greater inter-cluster interactions than IM, and hence a greater number of conductive pathways. The presence of these multiple pathways, expected in percolated CNT

systems, contributes to the lack of a significant change in resistivity as a function of T_c.

Young's moduli of IM specimens were consistently higher than those of CM specimens. No significant changes in modulus were observed with variations in T_c. The presence of CNTs stiffened the base matrix and changed the mode of failure from ductile in unfilled PC to brittle. The modulus of IM PC-MWCNT is within the range predicted by the modified Halpin–Tsai equations assuming randomly oriented and perfectly oriented CNTs. The modulus of CM PC-MWCNT is ~10% lower than that predicted due to the greater degree of CNT agglomeration visible in the micrographs.

Variations in both surface hardness and tensile strength with secondary processes and T_c were minor. The addition of CNTs to unfilled PC increases hardness by up to 4%. Hardness of IM specimens was ~3% lower than of CM specimens, likely due to the less established CNT network achieved in IM specimen surfaces. The moderate increases in hardness are attributed to ineffective filler-matrix stress transfer and matrix-rich regions. These same factors lead to the change in failure mechanism from ductile to brittle relative to unfilled PC, since CNT agglomerates may act as stress concentrations.

Examination of linear correlations between the solid-state properties generally yielded weak correlations. The most significant were: between hardness and resistivity for CM materials (negative), and between modulus and hardness (positive) for IM materials. The first was attributed to the distribution of filler agglomerates, with a greater number of matrix-rich regions giving rise to a lower hardness and conductivity. The second may be due to flow-induced orientation of nanotubes near the surface, as observed by other authors.

In summary, the findings suggest that the secondary process plays the crucial role in tailoring the final properties. The difference is primarily due to the timescales available for CNT agglomeration experienced in the secondary processes. High electrical conductivity is achieved with a time-dependent build-up of a CNT network, rendering fast industrial production of conductive nanocomposites a challenge. The changes in T_c had only a limited effect on the final properties, and this is widely attributed to the percolated nature of the materials studied here. Although this may be a useful lack of sensitivity for industrial processes, it is worth bearing in mind that primary processes play a greater role in unpercolated systems.[7]

REFERENCES

1. Krause, B.; Mende, M.; Pötschke, P.; Petzold, G. *Carbon* **2010**, *48*, 2746.
2. Pegel, S.; Pötschke, P.; Petzold, G.; Alig, I.; Dudkin, S. M.; Lellinger, D. *Polymer* **2008**, *49*, 974.
3. Pötschke, P.; Bhattacharyya, A. R.; Janke, A.; Pegel, S.; Leonhardt, A.; Täschner, C.; Ritschel, M.; Roth, S.; Hornbostel, B.; Cech, J. *Fullerenes Nanotubes Carbon Nanostruct.* **2005**, *13*, 211.
4. Bauhofer, W.; Kovacs, J. Z. *Compos. Sci. Technol.* **2009**, *69*, 1486.
5. Alig, I.; Pötschke, P.; Lellinger, D.; Skipa, T.; Pegel, S.; Kasaliwal, G. R.; Villmow, T. *Polymer* **2012**, *53*, 4.
6. Jamali, S.; Paiva, M. C.; Covas, J. A. *Polym. Test.* **2013**, *32*, 701.
7. Kasaliwal, G.; Göldel, A.; Pötschke, P. *J. Appl. Polym. Sci.* **2009**, *112*, 3494.
8. Kasaliwal, G. R.; Villmow, T.; Pegel, S.; Potschke, P. In Polymer - Carbon Nanotube Composites: Preparation, Properties and Applications; McNally, T., Potschke, P., Eds.; Woolhead publishings: Cambridge, **2011**; pp 92–132.
9. Zeiler, R.; Handge, U. A.; Dijkstra, D. J.; Meyer, H.; Altstädt, V. *Polymer* **2010**, *52*, 430.
10. Kasaliwal, G. R.; Pegel, S.; Göldel, A.; Pötschke, P.; Heinrich, G. *Polymer* **2010**, *51*, 2708.
11. Lew, C. Y.; Dewaghe, C.; Claes, M. In Polymer - Carbon Nanotube Composites: Preparation, Properties and Applications; McNally, T., Potschke, P., Eds.; Woolhead publishings: Cambridge, **2011**; pp 155–192.
12. Rios, P. F.; Ophir, A.; Kenig, S.; Efrati, R.; Zonder, L.; Popovitz-Biro, R. *J. Appl. Polym. Sci.* **2011**, *120*, 70.
13. Villmow, T.; Pegel, S.; Pötschke, P.; Wagenknecht, U. *Compos. Sci. Technol.* **2008**, *68*, 777.
14. Lellinger, D.; Xu, D.; Ohneiser, A.; Skipa, T.; Alig, I. *Phys. Status Solidi* **2008**, *245*, 2268.
15. Pegel, S.; Pötschke, P.; Villmow, T.; Stoyan, D.; Heinrich, G. *Polymer* **2009**, *50*, 2123.
16. Mack, C.; Sathyanarayana, S.; Weiss, P.; Mikonsaari, I.; Hübner, C.; Henning, F.; Elsner, P. *IOP Conf. Ser.: Mater. Sci. Eng.* **2012**, *40*, 012020.
17. Makrolon 2205 and 2207 Polycarbonate Resins, Technical Information, Edition 2009-05-11, Bayer MaterialScience AG, Leverkusen, Germany, **2009**.
18. Choong, G. Y. H.; De Focatiis, D. S. A.; Hassell, D. G. *Rheol. Acta* **2013**, *52*, 801.
19. Krause, B.; Boldt, R.; Pötschke, P. *Carbon* **2011**, *49*, 1243.
20. EN ISO 527-2:2012, Plastics - Determination of tensile properties In Part 2: Test conditions for moulding and extrusion plastics, BSI: London, **2012**.
21. De Focatiis, D. S. A. *Polym. Test.* **2012**, *31*, 550.
22. Pegel, S.; Villmow, T.; Pötschke, P. In Polymer - carbon nanotube composites: preparation, properties and applications; McNally, T., Potschke, P., Eds.; Woolhead publishings: Cambridge, **2011**; pp 265.
23. Krause, B.; Pötschke, P.; Häußler, L. *Compos. Sci. Technol.* **2009**, *69*, 1505.
24. Villmow, T.; Pötschke, P.; Pegel, S.; Häussler, L.; Kretzschmar, B. *Polymer* **2008**, *49*, 3500.
25. Choong, G. Y. H. A study of melt-compounded nanocomposites of polycarbonate and carbon nanotubes in the melt and solid states. Ph.D. Thesis, University of Nottingham, Nottingham, July **2014**.
26. Berger, H. H. *J. Electrochem. Soc.* **1972**, *119*, 507.
27. Tietjen, G. L.; Roger, M. H. *Technometrics* **1972**, *14*, 16.

28. Richter, S.; Saphiannikova, M.; Jehnichen, D.; Bierdel, M.; Heinrich, G. *eXPRESS Polym. Lett.* **2009**, *3*, 753.

29. Spikowski, J. M.; Kunzelman, J. In ANTEC 2012 Plastics: Annual Technical Conference Proceedings; Society of Plastics Engineers: Orlando, Florida, **2012**.

30. Lew, C. Y.; Xia, H.; McNally, T.; Fei, G.; Vargas, J.; Millar, B.; Douglas, P.; Claes, M.; Luizi, F. In Polymer Processing Society Europe/Africa Region Meeting, Larnaca; Polymer Processing Society: Cyprus, **2009**.

31. Liu, S.-P.; Hwang, S.-S.; Yeh, J.-M.; Pan, K.-W. *Int. Commun. Heat Mass Transf.* **2010**, *37*, 809.

32. Thostenson, E. T.; Chou, T.-W. *J. Phys. D: Appl. Phys.* **2003**, *36*, 573.

33. Gojny, F. H.; Wichmann, M. H. G.; Köpke, U.; Fiedler, B.; Schulte, K. *Compos. Sci. Technol.* **2004**, *64*, 2363.

34. Engels, T. A.; Govaert, L. E.; Meijer, H. E. *Macromol. Mater. Eng.* **2009**, *294*, 821.

35. Bhuiyan, M. A.; Pucha, R. V.; Worthy, J.; Karevan, M.; Kalaitzidou, K. *Compos. Struct.* **2013**, *95*, 80.

36. Pan, Z. W.; Xie, S. S.; Lu, L.; Chang, B. H.; Sun, L. F.; Zhou, W. Y.; Wang, G.; Zhang, D. L. *Appl. Phys. Lett.* **1999**, *74*, 3152.